AIAA Guidance, Navigation, and Control Conference and Exhibit
21 - 24 August 2006, Keystone, Colorado

AIAA 2006-6350

Neural Network Augmented Kalman Filtering in the Presence of Unknown System Inputs

Ramachandra J. Sattigeri [*]
School of Aerospace Engineering, Georgia Institute of Technology, Atlanta, GA 30332-0150

Anthony J. Calise[†]
School of Aerospace Engineering, Georgia Institute of Technology, Atlanta, GA 30332-0150

We present an approach for augmenting a linear, time-varying Kalman filter with an adaptive neural network (NN) for the state estimation of systems with linear process models acted upon by unknown inputs. The application is to the problem of tracking maneuvering targets. The unknown system inputs represent the effect of unmodeled disturbances acting on the system and are assumed to be continuous and bounded. The NN is trained online to estimate the unknown inputs. The training signal for the NN consists of two error signals. The first error signal is the residual of the Kalman filter that is augmented with the NN output. The second error signal is obtained after deriving a linear parameterization model of available system signals in terms of the ideal, unknown NN weights that linearly parameterize the unknown system inputs. The combination of two different sources of error signals to train the NN represents a composite adaptation type approach to adaptive state estimation. The approach is applied in a vision-based formation flight simulation of a leader and a follower unmanned aerial vehicle (UAV). The adaptive estimator onboard the follower UAV estimates the range, azimuth angle, and elevation angle to the leader UAV, the derivatives of these LOS variables, and the unknown leader aircraft acceleration along the axes of the Cartesian coordinate inertial frame. Simulation results with the presented approach are greatly improved when compared to those obtained with just a linear, time-varying Kalman filter and a particular adaptive state estimation method that utilizes just one source of error signals to train the NN [17].

I. Introduction

THE problem of tracking maneuvering targets has received a considerable degree of research effort over the decades in the field of estimation. The primary objective of target tracking is to estimate the state trajectories of a moving object. One of the major challenges for target tracking arises from target motion uncertainty. This uncertainty refers to the fact that an accurate dynamic model of the target being tracked is not available to the tracker. Specifically, even though the general form of the model is known, the tracker lacks knowledge about the actual control input of the target, also referred to as the target maneuver. In addition, any measurements of the target being tracked are corrupted by noise and time delays. A Kalman filter is usually used in the tracking problem but its performance may be seriously degraded unless the estimation error due to unknown target maneuvers is compensated. Two different approaches have been widely used to handle the case of unknown target maneuvers: model-based adaptive filtering and input estimation.

Various mathematical models of target motion have been developed over the past three decades. The models may: 1) approximate the actually nonrandom target maneuver as a random process of certain properties, or 2) describe typical target trajectories by some representative motion models with properly designed parameters. In the class of models where the target maneuver is modeled as a random process, the simplest model is the so-called white-noise acceleration model [1]. This model assumes that the target acceleration is an independent, white noise process. The intensity of this white noise can be adjusted online, which is the basis of some adaptive Kalman filter based target tracking algorithms [2-4]. Ref. [2] suggested a method in which the process noise covariance matrix can be estimated from the lagged prediction error covariance. This estimate is then directly utilized to compute the Kalman gain. Ref. [3] suggested techniques to independently estimate both the measurement noise covariance matrix and the process noise covariance matrix. The process noise covariance matrix is estimated by adjusting its value such that the statistics of the filter residual approach those of the optimum Kalman filter. Ref. [4] provided a procedure for

[*]Graduate Research Assistant, School of Aerospace Engineering, gte334x@prism.gatech.edu, AIAA Member.
[†] Professor, School of Aerospace Engineering, anthony.calise@ae.gatech.edu, Fellow AIAA.

adaptive computation of the process noise covariance matrix in an EKF for ballistic target tracking. The second next simplest model for target maneuver is the so-called white noise jerk model [1], which assumes that the derivative of the acceleration of the target is an independent, white noise process. While the white noise models have the advantage of simplicity, they rarely capture to a sufficient degree the full range of maneuvers that targets are capable of performing. For many applications, a better approach is to use Markov process models. An example is the Singer model [5] which assumes that the target acceleration is a zero-mean first-order stationary Markov process. This formulation of the target maneuver model suppresses the bias in the state estimates to a certain degree but can exhibit poorer performance than simpler models when there is no target maneuver. More sophisticated approaches include the variable-dimension filter approach [6] in which extra states are introduced in the filter when an input is detected and the interacting multiple model (IMM) technique [7] in which the change of the plant is modeled as a Markovian parameter having a transition probability. Kinematic approaches to modeling the target maneuver include the circular motion model [8] and the more general curvilinear motion model [9]. Another technique has been to incorporate kinematic constraints as a pseudo-measurement in the Kalman filter [10]. An example of kinematic constraint is that the acceleration vector is always perpendicular to the velocity vector for a constant speed target. A comprehensive survey on target tracking using target models is given in Ref. [11]. In general for the model-based approaches to target state estimation, filter performance may not be satisfactory when the target maneuver does not comply with the model, and every approach can be defeated with a suitably chosen target maneuver.

Input estimation is a different approach in which the existence of target maneuvers is first detected and then the magnitude of the target maneuver (input) is estimated [12-15]. Ref. [12] proposes an input estimation technique using the least-squares method to calculate the input magnitude. Ref. [13] derives a recursive input estimation technique based on multiple-model filtering. Ref. [14] proposes a technique in which the unknown target maneuver is modeled as a linear combination of basis functions, which are some elementary functions of time. The coefficients of each basis function are estimated. Ref. [15] employs a constant velocity filter, an input estimator and a maneuver detector implemented in parallel. This filter structure is similar to that of the two-stage Kalman filter [16] where the target acceleration is treated as a "bias" term. In the two-stage Kalman filter approach, two filters are implemented in parallel. A constant velocity filter represents the "bias-free" filter and the acceleration filter represents the "bias" filter [16].

Ref. [17] presents an approach for augmenting an Extended Kalman Filter (EKF) with a NN for adaptive state estimation of uncertain nonlinear systems. The NN is trained online with the residuals of the EKF and is designed to estimate the unknown target maneuvers in real-time and compensate the EKF. However, in a particular application of this approach, we found it difficult to identify a fixed set of NN design parameters that could give reasonable target acceleration estimates for varying target maneuvers. This in turn gave rise to state estimation errors that were larger than expected. One possible explanation is that the residuals of the EKF used to train the NN online do not contain sufficient information.

The contribution of this paper is to modify the approach of Ref. [17] by deriving an additional error signal to train the NN. We assume that the target acceleration is linearly parameterized in terms of an ideal set of NN weights. This is similar to the assumption in Ref. [14], except that the basis functions in our approach are sigmoidal functions of the vector of delayed values of the output. We then derive a linear parameterization model in terms of available system signals and the ideal, but unknown, NN weights. Replacing the ideal NN weights with their estimates in the linear parameterization model provides an estimate of the "system output". The difference between the "system output" and its estimate is the additional error signal that is utilized to train the NN. Our approach is similar in spirit to the composite adaptation approach [18], the combined direct and indirect adaptive control approach [19] and the Q-mod approach to adaptive control [20] that employ additional error signals to improve the performance of the adaptive component in the system. The difference is that the approaches in Ref. [18]-[20] were applied to adaptive control problems with state feedback, while we apply the approach to an adaptive state estimation problem. The benefits of using an additional error signal to train the NN are clearly evident in the simulation results. The results show that the target acceleration can be estimated to a reasonably accurate degree and the state estimation errors are much smaller when compared to the case when there is no adaptation (nominal case, simple Kalman filter with white noise modeling of the target acceleration) and the case when the adaptive law in Ref. [17] is applied. Most important is the fact that the performance does not change significantly over varying target maneuvers. When compared to Ref. [17], our approach is limited thus far to state estimation of systems with linear process models. Ref. [28] provides another approach to adaptive state estimation in the presence of bounded disturbances and time-varying parameters. Neural networks are employed to approximate state and control-dependent continuous functional uncertainties and adaptive bounding technique is used to reject the effect of bounded disturbances.

The paper is organized as follows. Section II presents theorems and definitions that are required in developing the theory for our approach. Section III presents the problem formulation and details the procedure utilized to derive the additional error signal to train the NN. Section IV presents the simulation results with discussion. Conclusions and future research directions are outlined in Section V.

II. Mathematical Preliminaries

Consider the nonlinear dynamical system

$$\dot{x} = f(t, x), \ x(t_0) = x_0 \tag{1}$$

where $f : [0, \infty) \text{ x } D \to R^n$ is continuously differentiable, $D = \{x \in R^n \mid \|x\| < r\}$, and the Jacobian matrix $\left[\frac{\partial f}{\partial x}\right]$ is bounded and Lipschitz on D, uniformly in t.

Definition 1 [21]: Let $x = 0$ be an equilibrium point for the nonlinear system in (1). The equilibrium point $x = 0$ is exponentially stable (ES) if

$$\|x(t)\| \le k\|x(t_0)\| e^{-\lambda(t-t_0)}, \ \ k > 0, \ \ \lambda > 0, \ \forall t \ge t_0 \ge 0, \ \forall \|x(t_0)\| < c \tag{2}$$

where c is a positive constant independent of t_0; and is globally exponentially stable (GES) if this condition is satisfied for any initial state.

Theorem 1 [21]: Let $x = 0$ be an equilibrium point for the nonlinear system in (1) where $f : [0, \infty) \text{ x } D \to R^n$ is continuously differentiable, $D = \{x \in R^n \mid \|x\| < r\}$, and the Jacobian matrix $\left[\frac{\partial f}{\partial x}\right]$ is bounded and Lipschitz on D, uniformly in t. Let k, λ and r_0 be positive constants with $r_0 < \frac{r}{k}$. Let $D_0 = \{x \in R^n \mid \|x\| < r_0\}$. Assume that the trajectory of the system satisfies

$$\|x(t)\| \le k\|x(t_0)\| e^{-\lambda(t-t_0)}, \ \ \forall t \ge t_0 \ge 0, \ \forall \|x(t_0)\| \in D_0 \tag{3}$$

Then there is a continuously differentiable function $V : [0, \infty) \text{ x } D_0 \to R$ that satisfies the inequalities

$$\begin{aligned} &c_1\|x\|^2 \le V(t, x) \le c_2\|x\|^2 \\ &\frac{\partial V}{\partial t} + \frac{\partial V}{\partial x} f(t, x) \le -c_3\|x\|^2 \\ &\left\|\frac{\partial V}{\partial x}\right\| \le c_4\|x\| \end{aligned} \tag{4}$$

for some positive constants c_1, c_2, c_3 and c_4.

Theorem 2 [21]*:* Let $x = 0$ be an equilibrium point for the nonlinear system in (1). Let $D_0 = \{x \in R^n \mid \|x\| < r_0\}$. Let $V : [0, \infty) \text{ x } D_0 \to R$ be a continuously differentiable function such that

$$W_1(x) \le V(t, x) \le W_2(x) \tag{5}$$

$$\dot{V}(t, x) = \frac{\partial V}{\partial t} + \frac{\partial V}{\partial x} f(t, x) \le 0 \tag{6}$$

$$\int_{t}^{t+\delta} \dot{V}(\tau,\phi(\tau,t,x))\, d\tau \le -\lambda V(t,x), \quad 0<\lambda<1 \tag{7}$$

$\forall t \ge 0,\ \ \forall x \in D_0$, for some $\delta > 0$, where $W_1(x)$ and $W_2(x)$ are continuous positive definite functions on D_0 and $\phi(\tau,t,x)$ is the solution of the system that starts at (t,x). Then, the origin is uniformly asymptotically stable (UAS). If all the assumptions hold globally and $W_1(x)$ is radially unbounded, then the origin is globally asymptotically stable (GAS). If $W_1(x) \ge k_1\|x\|^c$, $W_2(x) \le k_2\|x\|^c$, $k_1 > 0$, $k_2 > 0$, $c > 0$, then the origin is ES.

Theorem 3 [22]*:* Assume that an n dimensional state vector $x(t)$ of an observable time-invariant system

$$\begin{aligned} \dot{x} &= f(x) \\ y &= h(x) \end{aligned} \tag{8}$$

evolves on an n dimensional ball of radius $\bar{r}$ in R^n, $B_{\bar{r}} = \{x \in R^n \mid \|x\| < \bar{r}\}$. Also assume that the system output $y(t) \in R^m$ and its derivatives up to the order $(n-1)$ are bounded. Then given arbitrary $\varepsilon^* > 0$, there exists a set of constant, bounded weights W and a positive time delay $d > 0$, such that the function $f(x)$ in (8) can be approximated over the compact set $B_{\bar{r}}$ by a linearly parameterized NN

$$f(x) = W^T \sigma(\bar{\mu}) + \varepsilon(\bar{\mu}), \ \ \|W\|_F \le W^*, \ \|\varepsilon(\bar{\mu})\| \le \varepsilon^* \tag{9}$$

using the input vector

$$\bar{\mu}(y(t),d) = \left[\Delta_d^{(0)} y^T(t) \ \dots \ \Delta_d^{(n-1)} y^T(t)\right] \in R^{nm} \tag{10}$$

where $\Delta_d^{(0)} y^T(t) = y^T(t)$, $\Delta_d^{(k)} y^T(t) = \dfrac{\Delta_d^{(k-1)} y^T(t) - \Delta_d^{(k-1)} y^T(t-d)}{d}$, $k = 1,2,\dots$, $\|\bar{\mu}\| \le \mu^*$, $\mu^* > 0$ is a uniform bound on $B_{\bar{r}}$.

III. Problem Formulation

Consider the following single-input-single-output (SISO) system

$$\begin{aligned} \dot{x} &= Ax + Bg(x,z), & x(0) &= x_0 \\ \dot{z} &= f_z(x,z), & z(0) &= z_0 \\ y &= Cx \end{aligned} \tag{11}$$

where $x \in D_x \subseteq R^{n_x}$ and $z \in D_z \subseteq R^{n_z}$ are the states of the system such that x represents the modeled states and z represents the unmodeled states, D_x and D_z are compact sets, $f_z(x,z) : R^{n_x} \times R^{n_z} \to R^{n_z}$ is an unknown, bounded function and represents the unmodeled dynamics, $g(x,z) : R^{n_x} \times R^{n_z} \to R$ is an unknown, uniformly bounded and continuous function and represents the way in which the unmodeled dynamics is coupled to the system dynamics, $y \in R$ represents the available measurement which is assumed to be bounded, the matrices (A,B,C) are known and the pair (A,C) is observable.

Remark 1: The unknown function $g(x,z)$ acts as the unknown system input or disturbance to the system with linear, time invariant process models given by the matrices (A,B,C).

A. Adaptive Estimator and Error Signal Derivation

Using Theorem 3, consider the following NN approximation of $g(x,z)$

$$g(x,z) = W^T\sigma(\bar{\mu}) + \varepsilon(\bar{\mu}), \|W\|_F \le W^*, \ \|\varepsilon(\bar{\mu})\| \le \varepsilon^* \tag{12}$$

where $\sigma(\bar{\mu}) = [\sigma_1(\bar{\mu}), \ldots, \sigma_N(\bar{\mu})]^T$ is a vector of sigmoidal functions $\sigma_i(\cdot)$, N is the number of neurons. The sigmoidal functions are uniformly bounded [24], that is, $|\sigma_i(\bar{\mu})| \le 1$.

Consider the following adaptive estimator to estimate the states of the system in (11):

$$\begin{aligned} \dot{\hat{x}}(t) &= A\hat{x}(t) + K(t)(y(t) - \hat{y}(t)) + B\nu_{ad}, \qquad \hat{x}(0) = \hat{x}_0 \\ \hat{y}(t) &= C\hat{x}(t) \end{aligned} \tag{13}$$

where $K(t)$ is the Kalman gain obtained through the following set of matrix differential Ricatti equations [23]

$$\begin{aligned} \dot{P}(t) &= AP(t) + P(t)A^T - P(t)C^T R^{-1} CP(t) + Q \\ K(t) &= P(t)C^T R^{-1} \end{aligned} \tag{14}$$

where $P(0) = P_0 > 0,\ Q = Q^T \ge 0,\ R = R^T > 0$. The solution $P(t)$ of (14) is bounded, symmetric, positive definite and continuously differentiable. The output of the NN ν_{ad} is given by

$$\nu_{ad} = \hat{W}(t)^T \sigma(\bar{\mu}) \tag{15}$$

where $\hat{W}(t)$ is the estimate of the weight vector W in (12). The NN output ν_{ad} is designed to approximate the bounded disturbance $g(x,z)$. The formulation so far replicates the formulation in Ref. [17] applied to the system in (11). The residual signal of the adaptive estimator $\tilde{y}(t) = y(t) - \hat{y}(t)$ is the first error signal that is used to train the NN.

Next, consider the derivation of the second error signal to train the NN. Consider the following non-adaptive estimator for the system in (11)

$$\begin{aligned} \dot{\hat{x}}_1(t) &= A\hat{x}(t) + K_1(t)(y(t) - \hat{y}_1(t)), \qquad \hat{x}_1(0) = \hat{x}_{10} \\ \hat{y}_1(t) &= C\hat{x}_1(t) \end{aligned} \tag{16}$$

where $\tilde{y}_1(t) = y(t) - \hat{y}_1(t)$ is the residual of the non-adaptive estimator in (16), $K_1(t)$ is the Kalman gain obtained through the following set of matrix differential Ricatti equations [23]

$$\begin{aligned} \dot{P}_1(t) &= AP_1(t) + P_1(t)A^T - P_1(t)C^T R_1^{-1} CP_1(t) + Q_1 \\ K_1(t) &= P_1(t)C^T R_1^{-1} \end{aligned} \tag{17}$$

where $P_1(0) = P_{10} = P_0 > 0,\ Q_1 = Q_1^T \ge 0,\ R_1 = R_1^T > 0$. The solution $P_1(t)$ of (17) is bounded, symmetric, positive definite and continuously differentiable. We can choose the design matrices Q_1 and R_1 to be different from Q and R respectively in (14).

Consider the estimation error dynamics of the non-adaptive estimator in (16). Define $\tilde{x}_1 = x - \hat{x}_1$ and $\overline{A}_1(t) = A - K_1(t)C$. Then we have the following estimation error dynamics

$$\begin{aligned} \dot{\tilde{x}}_1 &= \overline{A}_1(t)\tilde{x}_1 + Bg(x,z) \\ \tilde{y}_1 &= C\tilde{x}_1 \end{aligned} \tag{18}$$

When $g(x,z) \equiv 0$, the estimation error dynamics can be shown to be GES. To see this consider the unforced estimation error dynamics in (19)

$$\begin{aligned} \dot{\tilde{x}}_1 &= \overline{A}_1(t)\tilde{x}_1 \\ \tilde{y}_1 &= C\tilde{x}_1 \end{aligned} \tag{19}$$

and the matrix differential equation (17). Eq. (17) can be re-written as

$$\dot{P}_1(t) = \overline{A}_1(t)P_1(t) + P_1(t)\overline{A}_1(t)^T + P_1(t)C^T R_1^{-1} C P_1(t) + Q_1 \tag{20}$$

which can be also written by invoking the identity $P_1(t)P_1(t)^{-1} = I$ and differentiating it:

$$\dot{P}_1(t)^{-1} = -P_1(t)^{-1}\overline{A}_1(t) - \overline{A}_1(t)^T P_1(t)^{-1} - \tilde{Q}_1(t) \tag{21}$$

$$\tilde{Q}_1(t) = C^T R_1^{-1} C + P_1(t)^{-1} Q_1 P_1(t)^{-1} \geq 0 \tag{22}$$

Now consider the Lyapunov candidate function $V_1(t,\tilde{x}_1) = \tilde{x}_1^T P_1(t)^{-1}\tilde{x}_1$. Since $P_1(t)$ is bounded, symmetric and positive definite, there exist positive constants ρ_1 and ρ_2, $\rho_1 > \rho_2 > 0$, such that

$$0 < \frac{1}{\rho_1}\|\tilde{x}_1\|^2 \leq V_1(t,\tilde{x}_1) \leq \frac{1}{\rho_2}\|\tilde{x}_1\|^2 \tag{23}$$

So $V_1(t,\tilde{x}_1)$ is decresent and radially unbounded [21]. Differentiating $V_1(t,\tilde{x}_1)$

$$\dot{V}_1(t,\tilde{x}_1) = \dot{\tilde{x}}_1^T P_1(t)^{-1}\tilde{x} + \tilde{x}_1^T P_1(t)^{-1}\dot{\tilde{x}} + \tilde{x}_1^T \dot{P}_1(t)^{-1}\tilde{x}_1 \tag{24}$$

Substituting for $\dot{\tilde{x}}_1$ from eq. (19) and $\dot{P}_1(t)^{-1}$ from eq. (21), eq. (24) simplifies to

$$\dot{V}_1(t,\tilde{x}_1) = -\tilde{x}_1^T \tilde{Q}_1(t)\tilde{x}_1 \leq 0 \tag{25}$$

where $\tilde{Q}_1(t)$ is given by eq. (22). Since $Q_1 \geq 0$, we have $P_1(t)^{-1}Q_1P_1(t)^{-1} \geq 0$. This implies that

$$\dot{V}_1(t,\tilde{x}_1) \leq -\tilde{x}_1^T C^T R_1^{-1} C\tilde{x}_1 \leq 0 \tag{26}$$

The solution of the linear time-varying system (19) starting at $(t,\tilde{x}_1)$ is given by

$$\phi(\tau,t,\tilde{x}_1) = \Phi(\tau,t)\tilde{x}_1(t) \tag{27}$$

where $\Phi(\tau,t)$ is the state transition matrix of the system (19). Therefore, we have for some $\delta > 0$,

$$\int_t^{t+\delta} \dot{V}_1\left(\tau, \phi\left(\tau, t, \tilde{x}_1\right)\right)\, d\tau \le -\tilde{x}_1^T \left[\int_t^{t+\delta} \Phi^T(\tau,t) L^T\, L\, \Phi(\tau,t) d\tau\right] \tilde{x}_1 = -\tilde{x}_1^T W_1(t,t+\delta)\tilde{x}_1 \tag{28}$$

where $L = R_1^{-1/2} C$. The matrix $W_1(t,t+\delta)$ is the observability gramian of the pair $\left(\overline{A}_1(t), L\right) = \left(A - P_1(t) C^T R_1^{-1}, R_1^{-1/2} C\right)$. Observability of the pair (A,C) guarantees uniform observability of the pair $\left(\overline{A}_1(t), L\right) = \left(A - P_1(t) C^T R_1^{-1}, R_1^{-1/2} C\right)$.

The above fact guarantees that $W_1(t,t+\delta) \ge kI > 0$, $\forall t \ge 0$, where $k < \dfrac{1}{\rho_2}$. This implies that

$$\int_t^{t+\delta} \dot{V}_1\left(\tau, \phi\left(\tau, t, \tilde{x}_1\right)\right)\, d\tau \le -k\left\|\tilde{x}_1\right\|^2 \le -k\rho_2 V_1\left(t, \tilde{x}_1\right) \tag{29}$$

Eq. (23), (25) and (29) satisfy the sufficient conditions (5)-(7) of Theorem 2 with $W_1\left(\tilde{x}_1\right) = \dfrac{1}{\rho_1}\left\|\tilde{x}_1\right\|^2$ and $W_2\left(\tilde{x}_1\right) = \dfrac{1}{\rho_2}\left\|\tilde{x}_1\right\|^2$. This implies that the origin $\tilde{x}_1(t) \equiv 0$ of the unforced system (19) is GES. Considering the time-domain solution of eq. (19), we have

$$\tilde{x}_1(t) = \Phi(t,t_0)\tilde{x}_1(t_0), \ \forall t \ge t_0 \ge 0 \tag{30}$$

Definition 1 now implies that

$$\left\|\tilde{x}_1(t)\right\| = \left\|\Phi(t,t_0)\tilde{x}_1(t_0)\right\| \le k\left\|\tilde{x}_1(t_0)\right\| e^{-\lambda(t-t_0)} \tag{31}$$

for some positive constants k and λ and for $\tilde{x}_1(t_0) \in R^n$. This implies that

$$\Phi(t,t_0)\tilde{x}_1(t_0) \to 0 \ \text{as} \ t \to \infty, \ \forall t \ge t_0 \ge 0 \tag{32}$$

Since the estimation error dynamics in eq. (19) are GES, in the presence of the bounded disturbance $g(x,z)$ the estimation error $\tilde{x}_1$, the state vector of the system in (18), is input-to-state stable [21]. This implies that $\tilde{x}_1(t)$ is bounded as long as $g(x,z)$ is bounded. This also implies that the residual $\tilde{y}_1(t)$ is bounded as long as $g(x,z)$ is bounded.

Eq. (18) can be written in terms of the linear parameterization of $g(x,z)$ in eq. (12) as

$$\begin{aligned} \dot{\tilde{x}}_1 &= \overline{A}_1(t)\tilde{x}_1 + BW^T\sigma(\overline{\mu}) + B\varepsilon \\ \tilde{y}_1 &= C\tilde{x}_1 \end{aligned} \tag{33}$$

where $\|W\|_F \le W^*$, $\|\varepsilon(\overline{\mu})\| \le \varepsilon^*$. The time domain solution for the residual $\tilde{y}_1$ is given by

$$\tilde{y}_1(t) = C\Phi(t,t_0)\tilde{x}_1(t_0) + \int_{t_0}^{t} C\Phi(t,\tau)BW^T\sigma(\overline{\mu})\, d\tau + \int_{t_0}^{t} C\Phi(t,\tau)B\varepsilon\, d\tau \tag{34}$$

where $\Phi(t,t_0)$ is the state transition matrix of the system in (33). Since $g(x,z)\in R$ and W is a constant vector, eq. (34) can be re-written as

$$\tilde{y}_1(t) = C\Phi(t,t_0)\tilde{x}_1(t_0) + \left[\int_{t_0}^{t} C\Phi(t,\tau)B\sigma^T(\overline{\mu})\, d\tau\right]W + \varepsilon_f(t,t_0) \tag{35}$$

where $\varepsilon_f(t,t_0)$ is the output of the following dynamical system,

$$\begin{aligned} \dot{x}_\varepsilon &= \overline{A}_1(t)x_\varepsilon + B\varepsilon, \quad x_\varepsilon(t_0) = 0 \\ \varepsilon_f &= Cx_\varepsilon \end{aligned} \tag{36}$$

and ε_f is always bounded since it is the output of the GES system in (19) with bounded input ε. Let $\left\|\varepsilon_f(t,t_0)\right\| \le \varepsilon_f^*$. Eq. (35) can now be written as

$$\tilde{y}_1(t) = C\Phi(t,t_0)\tilde{x}_1(t_0) + q(t,t_0)W + \varepsilon_f(t,t_0) \tag{37}$$

where $q(t,t_0)$ is a row vector given by

$$q(t,t_0) = \left[\sigma_{f1}(t,t_0)\sigma_{f2}(t,t_0)\ldots\sigma_{fN}(t,t_0)\right] \tag{38}$$

and the $\sigma_{fi}(t,t_0)$, $i = 1,2,\ldots,N$ are the outputs of the GES system in (19) with uniformly bounded inputs $\sigma_i(\overline{\mu})$, $i = 1,2,\ldots,N$, i.e.,

$$\begin{aligned} \dot{x}_{fi} &= \overline{A}_1(t)x_{fi} + B\sigma_i(\overline{\mu}(t)), \quad x_{fi}(t_0) = 0,\ i = 1,2,\ldots,N \\ \sigma_{fi} &= Cx_{fi} \end{aligned} \tag{39}$$

The boundedness of $\sigma_i(\overline{\mu})$ implies the boundedness of $\sigma_{fi}(t,t_0)$ which in turn implies the boundedness of the row vector $q(t,t_0)$. The initial condition $\tilde{x}_1(t_0)$ and the filtered NN approximation error $\varepsilon_f(t,t_0)$ are not available.

Eq. (37) is a linear parameterization model in terms of the available residual signal $\tilde{y}_1(t)$ and the unknown, constant NN weight vector W. Consider an estimate of the residual $\tilde{y}_1(t)$ by replacing W by its estimate $\hat{W}(t)$

$$\hat{\tilde{y}}_1(t) = q(t,t_0)\hat{W}(t) \tag{40}$$

The signal formed by the difference between $\tilde{y}_1(t)$ and $\hat{\tilde{y}}_1(t)$ is the second error signal used to train the NN and is given by

$$e_1(t) = \tilde{y}_1(t) - \hat{\tilde{y}}_1(t) = \tilde{y}_1(t) - q(t,t_0)\hat{W}(t) \tag{41}$$

Remark 2: It requires $(N+1)$ time-varying filters (Eq. 16 and 39) to generate the error signal $e_1(t)$.

Let the NN adaptive law be given by

$$\dot{\hat{W}} = -\Gamma_W \left\{ -\sigma(\bar{\mu})\tilde{y} - \gamma_W q^T(t, t_0) e_1 + \lambda_W \hat{W} \right\} \tag{42}$$

with the NN design constants $\Gamma_W > 0$, $\gamma_W > 0$ and $\lambda_W > 0$, where Γ_W and γ_W are adaptation gains and λ_W is the sigma-mod parameter [25].

Remark 3: The form of the adaptive law containing the error term $e_1(t)$ is the gradient descent approach [18] to minimizing $e_1(t)$. Other potential approaches include the standard least-squares minimization, least-squares with exponential forgetting [18], etc.

IV. Simulation Results

We consider the 6 DOF leader-follower formation flight configuration [26] to illustrate the simulation results. The leader aircraft in Ref. [26] is the maneuvering target to be tracked. The leader aircraft tracks waypoints in the inertial 3D space. The waypoints can be arranged so as to result in various target maneuvers. For example, in this paper we consider two specific target maneuvers. The first target maneuver is the square-box trajectory maneuver. This maneuver is generated by making the target aircraft track waypoints at the corners of a square box in the horizontal plane. This maneuver is characterized by sharp heading changes at the corners of the square box followed by larger segments of constant velocity flight. The second target maneuver is a circular trajectory maneuver. This maneuver is generated by making the target aircraft track waypoints on a circle in the horizontal plane. The resulting target maneuver is a smaller amplitude maneuver than the square-box trajectory maneuver but the duration of constant velocity flight is much reduced in this case. The two maneuvers are thus different from each other and can be used to check the consistency of performance of the adaptive state estimation method presented in the previous sections.

The follower aircraft tracks the leader aircraft for a commanded range of 5 meters [26]. Since the approach presented in the previous sections is applicable for adaptive state estimation only, we do not use the state estimates in the guidance law. We implement the guidance law in Ref. [26] that assumes true values of the range R, LOS azimuth angle λ_A and LOS elevation angle λ_E are available. We consider the LOS kinematics in the inertial Cartesian coordinate frame

$$\frac{d}{dt}\begin{bmatrix} R_X \\ \dot{R}_X \\ R_Y \\ \dot{R}_Y \\ R_Z \\ \dot{R}_Z \end{bmatrix} = \underbrace{\begin{bmatrix} 0 & 1 & 0 & 0 & 0 & 0 \\ 0 & 0 & 0 & 0 & 0 & 0 \\ 0 & 0 & 0 & 1 & 0 & 0 \\ 0 & 0 & 0 & 0 & 0 & 0 \\ 0 & 0 & 0 & 0 & 0 & 1 \\ 0 & 0 & 0 & 0 & 0 & 0 \end{bmatrix}}_{A} \begin{bmatrix} R_X \\ \dot{R}_X \\ R_Y \\ \dot{R}_Y \\ R_Z \\ \dot{R}_Z \end{bmatrix} + \underbrace{\begin{bmatrix} 0 & 0 & 0 \\ 1 & 0 & 0 \\ 0 & 0 & 0 \\ 0 & 1 & 0 \\ 0 & 0 & 0 \\ 0 & 0 & 1 \end{bmatrix}}_{B} \begin{bmatrix} a_{T_X} \\ a_{T_Y} \\ a_{T_Z} \end{bmatrix} + \begin{bmatrix} 0 & 0 & 0 \\ 1 & 0 & 0 \\ 0 & 0 & 0 \\ 0 & 1 & 0 \\ 0 & 0 & 0 \\ 0 & 0 & 1 \end{bmatrix} \begin{bmatrix} -a_{F_X} \\ -a_{F_Y} \\ -a_{F_Z} \end{bmatrix} \tag{46}$$

where R_X, R_Y and R_Z are respectively the projections of the range vector from the follower to the target aircraft onto the inertial X, Y and Z axes, and the subscripts T and F refer to target (leader) and follower aircraft respectively. We assume that there is a vision sensor onboard the follower aircraft that can measure the subtended angle α, the azimuth angle λ_A, and the elevation angle λ_E with zero-mean additive measurement white noise of standard deviation 0.01 radians for each measurement [27]. The subtended angle measures the maximum size subtended by the target aircraft on the follower image plane. Using these raw measurements, we can create pseudo-measurements of R_X, R_Y and R_Z using the relationship between subtended angle, azimuth angle and elevation angle and range [27]

$$
\begin{aligned}
R_m &= \frac{b}{2\tan\left(\frac{\alpha_m}{2}\right)} \\
R_{X_m} &= R_m \cos\left(\lambda_{A_m}\right)\cos\left(\lambda_{E_m}\right) \\
R_{Y_m} &= R_m \sin\left(\lambda_{A_m}\right)\cos\left(\lambda_{E_m}\right) \\
R_{Z_m} &= -R_m \sin\left(\lambda_{E_m}\right)
\end{aligned}
\tag{47}
$$

where the subscript m indicates the variables are measurements, and b is the target size (wing-span length), assumed constant and known for this simulation. The conversion of the image plane noisy measurements of α, λ_A and λ_E into the measurements of R_X, R_Y and R_Z allows us to use the following linear, measurement model for the LOS kinematics in (46)

$$
\underbrace{\begin{bmatrix} y_1 \\ y_2 \\ y_3 \end{bmatrix}}_{Y} = \underbrace{\begin{bmatrix} 1 & 0 & 0 & 0 & 0 & 0 \\ 0 & 0 & 1 & 0 & 0 & 0 \\ 0 & 0 & 0 & 0 & 1 & 0 \end{bmatrix}}_{C} \underbrace{\begin{bmatrix} R_X \\ \dot{R}_X \\ R_Y \\ \dot{R}_Y \\ R_Z \\ \dot{R}_Z \end{bmatrix}}_{X} + \begin{bmatrix} \nu_X \\ \nu_Y \\ \nu_Z \end{bmatrix}
\tag{48}
$$

where ν_X, ν_Y and ν_Z are now state-dependent measurement noise terms. We evaluate the adaptive state estimation approach on the basis of estimation accuracy of the range R, range-rate $\dot{R}$, azimuth rate $\dot{\lambda}_A$, elevation rate $\dot{\lambda}_E$, and the target acceleration $\left[a_{T_X},\ a_{T_Y},\ a_{T_Z}\right]^T$. These variables are the most important from point of view of implementation in the guidance law, which is the next step after estimation. The range, range-rate, azimuth rate and elevation rate terms are related to the states of the LOS kinematics model in eq. (46) through the following relations

$$
\begin{aligned}
R &= \sqrt{R_X^2 + R_Y^2 + R_Z^2} \\
\dot{R} &= \frac{R_X \dot{R}_X + R_Y \dot{R}_Y + R_Z \dot{R}_Z}{R}
\end{aligned}
\tag{49}
$$

$$
\begin{aligned}
\lambda_A &= \tan^{-1}\left(\frac{R_Y}{R_X}\right) \\
\dot{\lambda}_A &= \frac{1}{\sqrt{R_X^2 + R_Y^2}}\left(\dot{R}_Y \cos\lambda_A - \dot{R}_X \sin\lambda_A\right)
\end{aligned}
\tag{50}
$$

$$
\begin{aligned}
\lambda_E &= -\sin^{-1}\left(\frac{R_Z}{R}\right) \\
\dot{\lambda}_E &= -\frac{1}{R}\left[\dot{R}_Z \cos\lambda_E + \dot{R}_X \cos\lambda_A \sin\lambda_E + \dot{R}_Y \sin\lambda_A \sin\lambda_E\right]
\end{aligned}
\tag{51}
$$

Note that even though the system in (46), (48) is multi-input multi-output (MIMO), each input-output channel is completely decoupled and we can use the theory developed in Sections II-IV for implementation.

A. Results with Linear, Time-Varying Kalman Filter (No Adaptation)

This section shows results obtained by using a linear, time-varying Kalman filter as the state estimator. The target acceleration components along the X, Y and Z axes are modeled as independent, zero-mean, white noise processes in the design of the filter. Figure 1 shows the range and the range-rate estimation error for the square-box trajectory target maneuver. The top sub-plot on the RHS is a plot of the true range-rate (red solid line) and the estimated range-rate (blue dashed line). The bottom sub-plot on the RHS is the range-rate estimation error in m/s. At time $t = 20, 40$ and 60 s, the target initiates a heading change and Figure 1 shows that the estimation errors peak just after these target maneuvers. The reasons for the peaking of the estimation errors is that the white-noise process models used in the design of the Kalman filter are in no way representative of the true target acceleration components along the X, Y and Z axes. The estimation errors go slowly towards zero when the target stops maneuvering. The simulation is stopped at about 84 seconds.

Figure 2 shows the azimuth rate and elevation rate estimation error for the square-box trajectory target maneuver. It is seen that the estimation error for both the LOS rates peaks just after the target initiates a heading change maneuver.

Next, we show results for the circular trajectory maneuver with the same Kalman filter. Figure 3 shows the range and the range-rate estimation error. Figure 4 shows the azimuth rate and elevation rate estimation error. The peaks in the estimation errors again correspond to a target heading change maneuver.

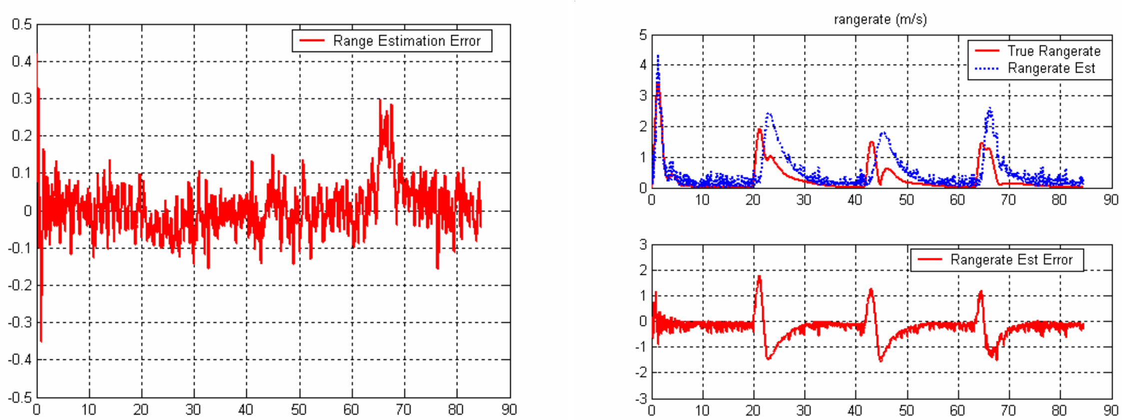

Figure 1. Range Estimation Error in meters (LHS), Range-rate Estimation Error in m/s (RHS), Square-box Trajectory Maneuver, No Adaptation

LHS = Left Hand Side, RHS = Right Hand Side

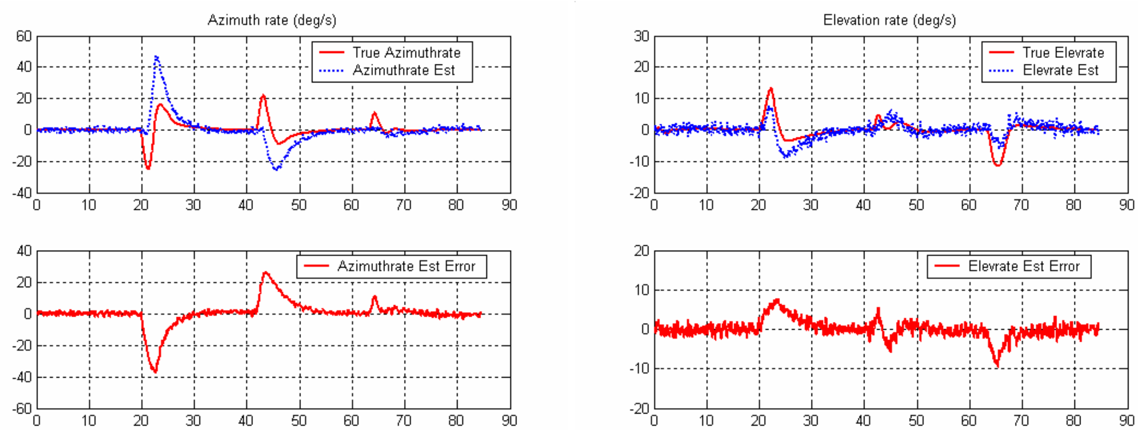

Figure 2. Azimuth Rate Estimation Error in deg/s (LHS), Elevation Rate Estimation Error in deg/s (RHS), Square-box Trajectory Maneuver, No Adaptation

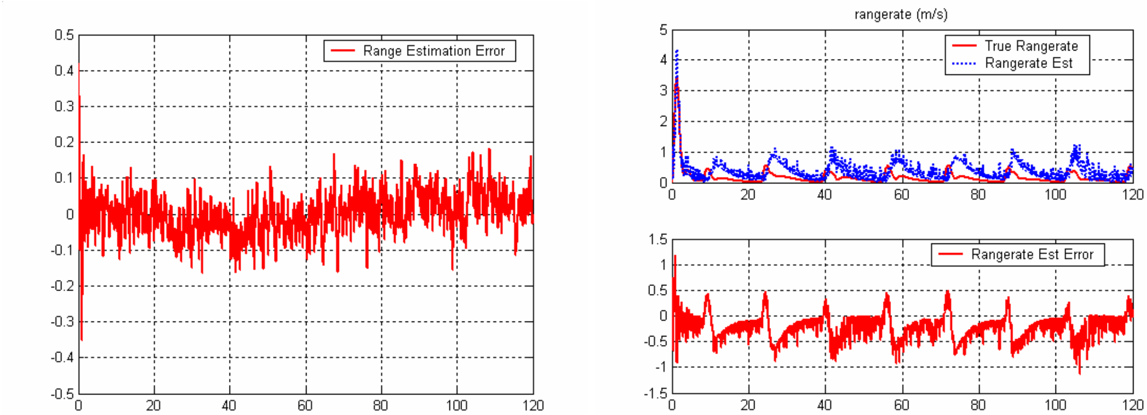

Figure 3. Range Estimation Error in meters (LHS), Range-rate Estimation Error in m/s (RHS), Circular Trajectory Maneuver, No Adaptation

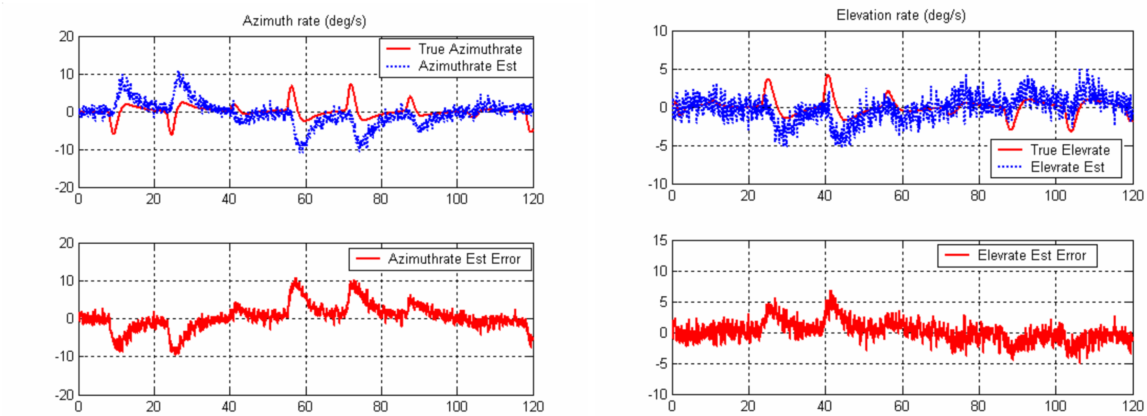

Figure 4. Azimuth Rate Estimation Error in deg/s (LHS), Elevation Rate Estimation Error in deg/s (RHS), Circular Trajectory Maneuver, No Adaptation

B. Results with Adaptive State Estimator in Ref. [17]

This section shows results obtained by augmenting the Kalman filter in Section V-A with a NN trained online with the adaptive law in Ref. [17]. Figure 5 shows the range and the range-rate estimation error for the square-box trajectory target maneuver. Figure 6 shows the azimuth rate and elevation rate estimation error for the square-box trajectory target maneuver. It is clear upon comparison with Figs. 1 and 2 that the performance of the adaptive estimator is slightly worse off than with just the linear Kalman filter. This can be seen by comparing the peaks of the estimation errors of the range, azimuth and elevation rates.

Figure 7 shows the target acceleration estimation performance for the square-box trajectory maneuver. The 3 sub-plots show the target acceleration estimation along the inertial X, Y and Z axes respectively. The true acceleration is shown in red, and the target acceleration estimate, which is the output of the NN, is shown by the blue dashed line in Figure 7. The reason why the state estimation performance is not much improved over that of the linear Kalman filter is because the target acceleration is not correctly captured by the NN.

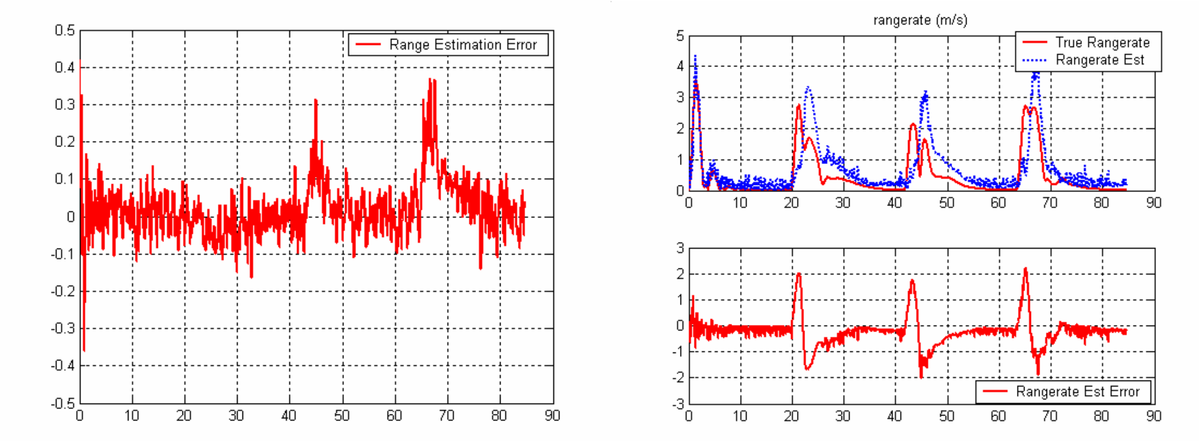

Figure 5. Range Estimation Error in meters (LHS), Range-rate Estimation Error in m/s (RHS), Square-box Trajectory Maneuver, Adaptive Estimator in Ref. [17]

LHS = Left Hand Side, RHS = Right Hand Side

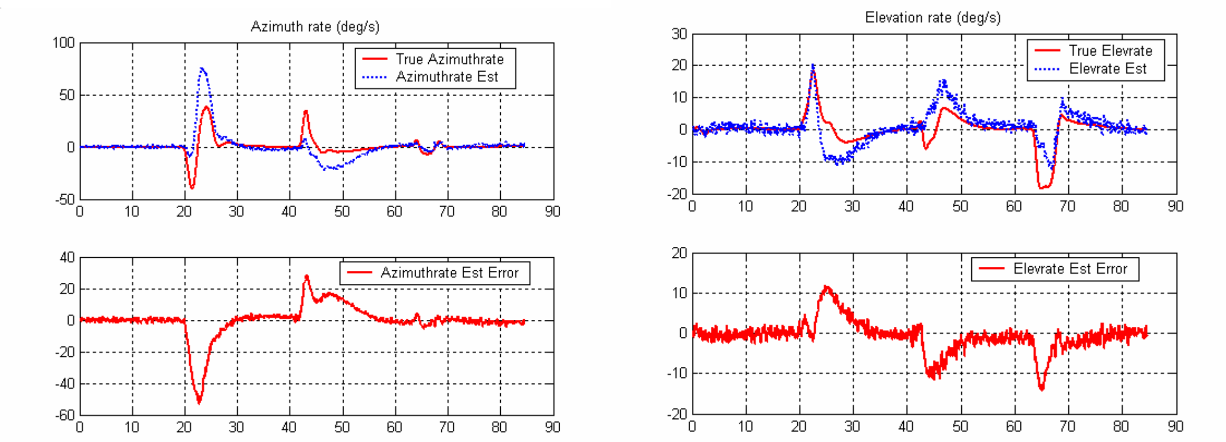

Figure 6. Azimuth Rate Estimation Error in deg/s (LHS), Elevation Rate Estimation Error in deg/s (RHS), Square-box Trajectory Maneuver, Adaptive Estimator in Ref. [17]

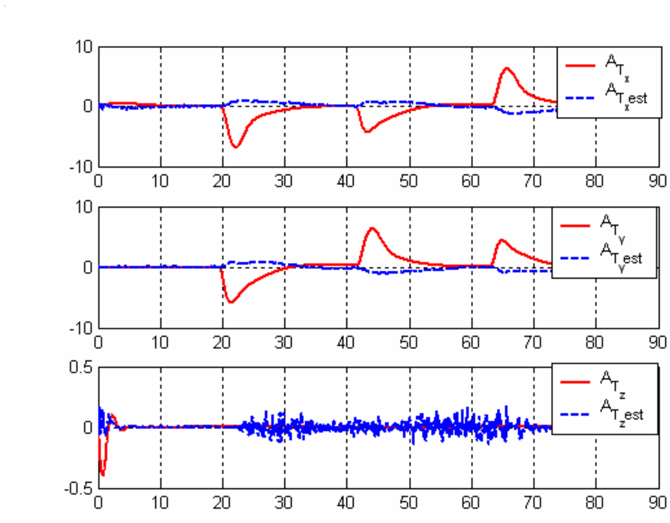

Figure 7. Target Acceleration Estimation in m/s^2, Square-box Trajectory Maneuver, Adaptive Estimator in Ref. [17]

Next, we show results for the circular trajectory maneuver with the same adaptive estimator. Figure 8 shows the range and the range-rate estimation error. Figure 9 shows the azimuth rate and elevation rate estimation error. Figure 10 shows the target acceleration estimation performance. The results again show that the estimation performance with the adaptive estimation is slightly worse off than with just the linear Kalman filter.

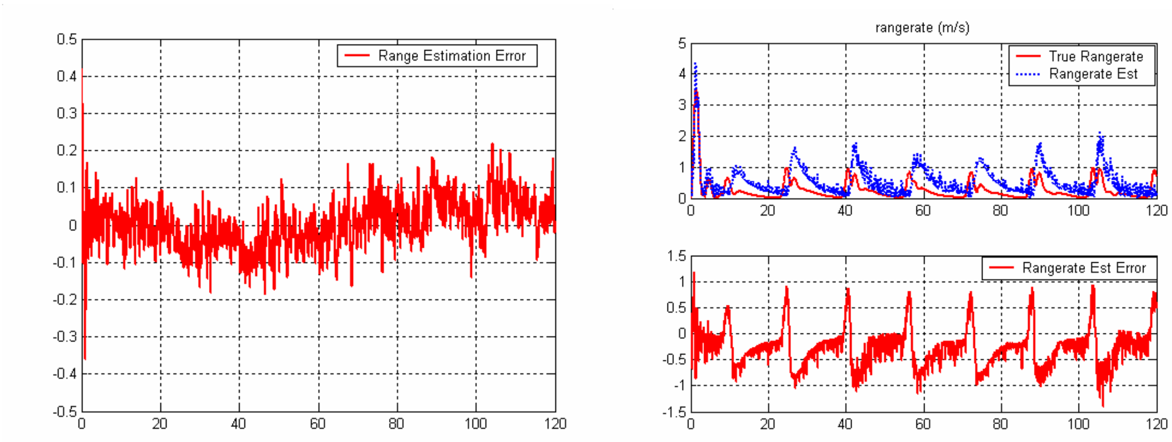

Figure 8. Range Estimation Error in meters (LHS), Range-rate Estimation Error in m/s (RHS), Circular Trajectory Maneuver, Adaptive Estimator in Ref. [17]

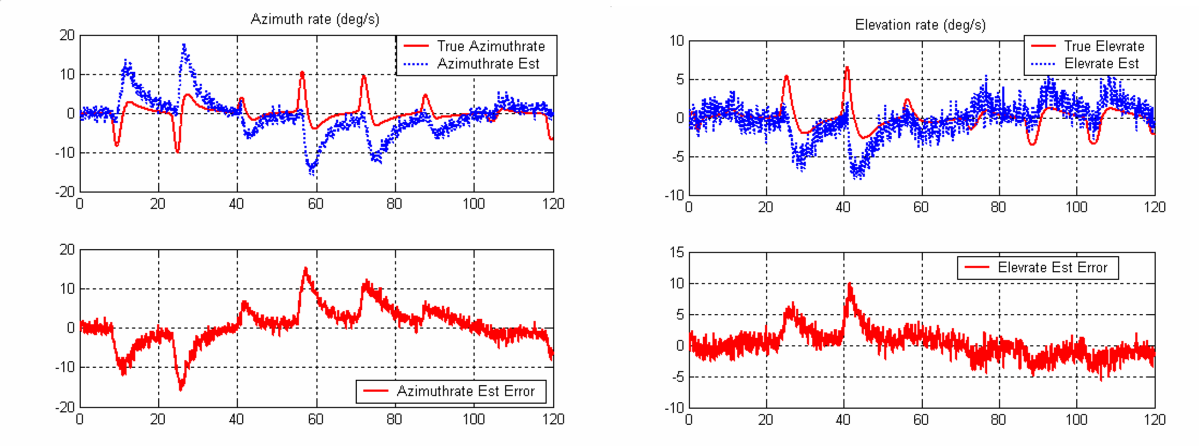

Figure 9. Azimuth Rate Estimation Error in deg/s (LHS), Elevation Rate Estimation Error in deg/s (RHS), Circular Trajectory Maneuver, Adaptive Estimator in Ref. [17]

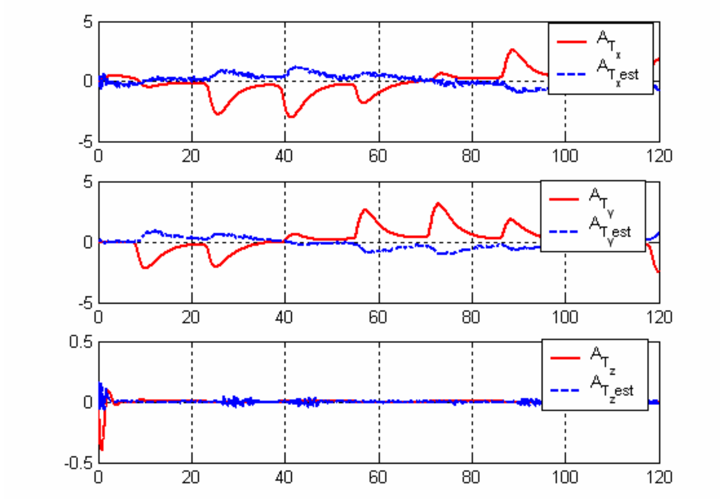

Figure 10. Target Acceleration Estimation in m/s^2, Circular Trajectory Maneuver, Adaptive Estimator in Ref. [17]

It can be clearly concluded that the inaccurate estimation of the target acceleration in Figures 7 and 10 leads to the estimation errors in Figures (5), (6), (8) and (9) respectively.

C. Results with Adaptive State Estimator formulated in this paper

In this section, the results are obtained by augmenting the Kalman filter with a NN that is trained with the adaptive law in Eq. (42). The following results are shown on the same scale as the results in Figures 1-10 to facilitate easier comparison.

Figure 11 shows the range and the range-rate estimation error for the square-box trajectory target maneuver. Comparing with the corresponding Figures 1 (no adaptation) and 5, it is seen that the peaks in the range estimation error and the range-rate estimation error are much smaller in Figure 11. Figure 12 shows the azimuth rate and elevation rate estimation error. Comparing Figure 12 with Figures 2 (no adaptation) and 6 shows the vastly improved performance with the adaptive state estimator presented in this paper.

Figure 13 shows the target acceleration estimation performance. The figure shows that the target acceleration estimates are reasonably accurate thus showing a major improvement when compared to the result in Figure 7. The acceleration estimates however are noisier when compared to the corresponding plot in Figure 7. The range-rate, azimuth-rate and elevation-rate estimation errors in Figures 11 and 12 are much smaller when compared to the corresponding plots in Figures 1 and 2 (no adaptation) and in Figures 5 and 6.

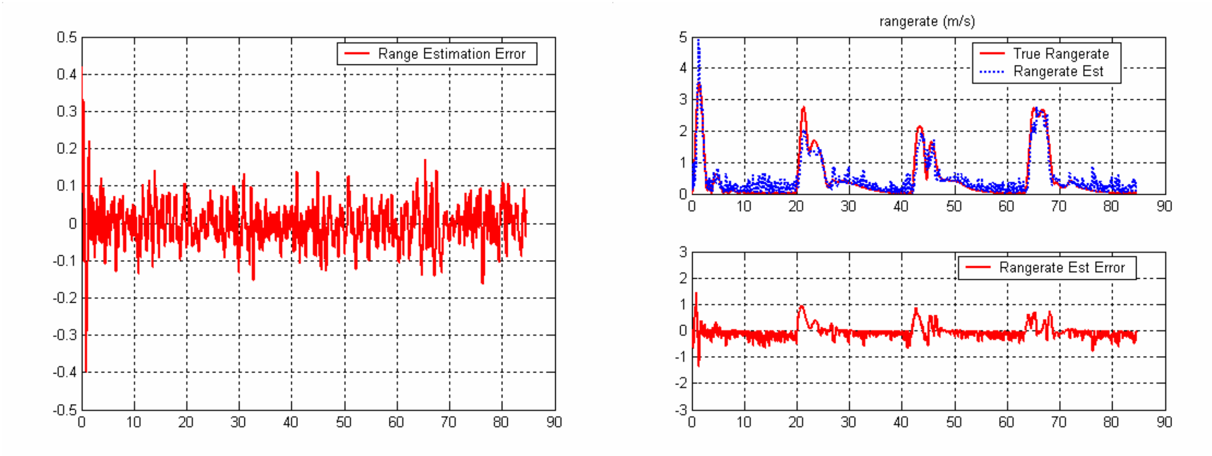

Figure 11. Range Estimation Error in meters (LHS), Range-rate Estimation Error in m/s (RHS), Square-box Trajectory Maneuver, Adaptive Estimator formulated in this paper

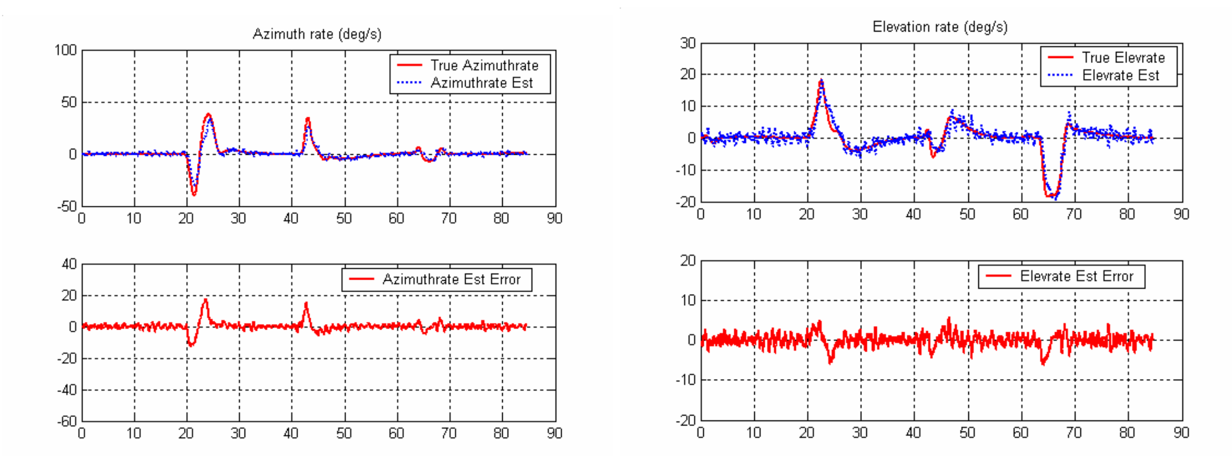

Figure 12. Azimuth Rate Estimation Error in deg/s (LHS), Elevation Rate Estimation Error in deg/s (RHS), Square-box Trajectory Maneuver, Adaptive Estimator formulated in this paper

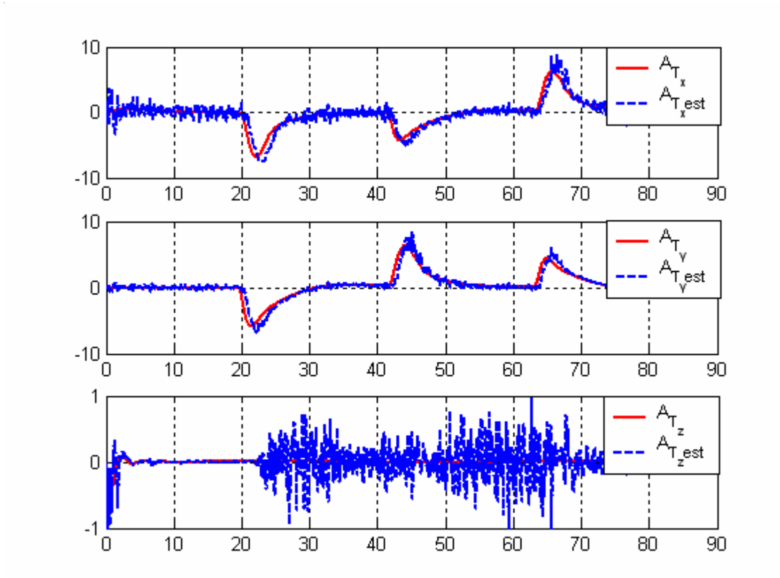

Figure 13. Target Acceleration Estimation in m/s^2, Square-box Trajectory Maneuver, Adaptive Estimator formulated in this paper

Figures 14-16 show results for the circular trajectory maneuver with the adaptive estimator formulated in this paper. These figures show that the estimation performance does not deteriorate when the target maneuver is changed.

Figure 14 shows the range and the range-rate estimation error. Figure 15 shows the azimuth rate and elevation rate estimation error. The peak estimation error is much smaller than the peak estimation error in Figures 3 (no adaptation) and 9. Estimation performance is consistent over the entire target maneuver.

Figure 16 shows the target acceleration estimation performance. Figure 16 again shows that the estimates of the target acceleration components are much more accurate than in Figure 10. However, these estimates are also very noisy when compared to the estimates in Figure 10. The most significant improvement comes in the estimation of the azimuth and elevation rates.

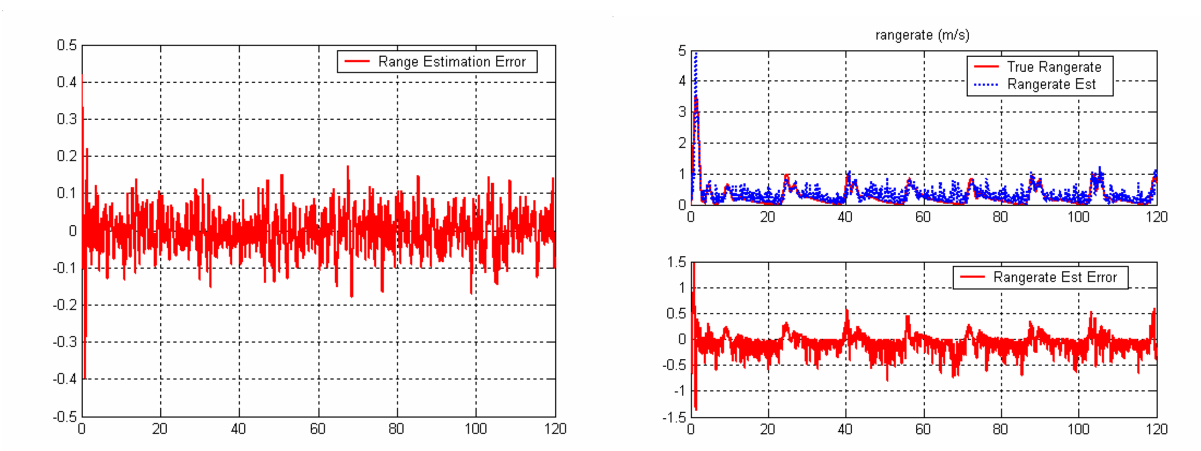

Figure 14. Range Estimation Error in meters (LHS), Range-rate Estimation Error in m/s (RHS), Circular Trajectory Maneuver, Adaptive Estimator formulated in this paper

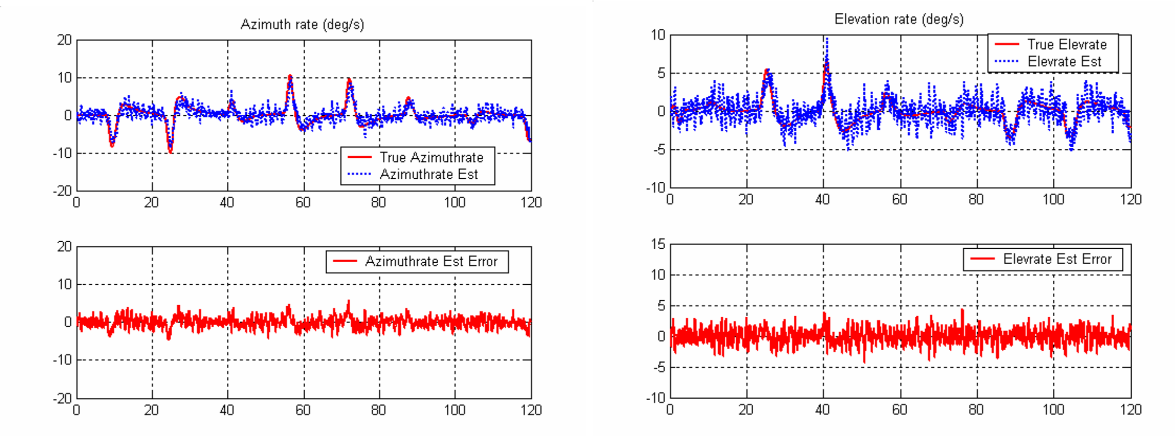

Figure 15. Azimuth Rate Estimation Error in deg/s (LHS), Elevation Rate Estimation Error in deg/s (RHS), Circular Trajectory Maneuver, Adaptive Estimator formulated in this paper

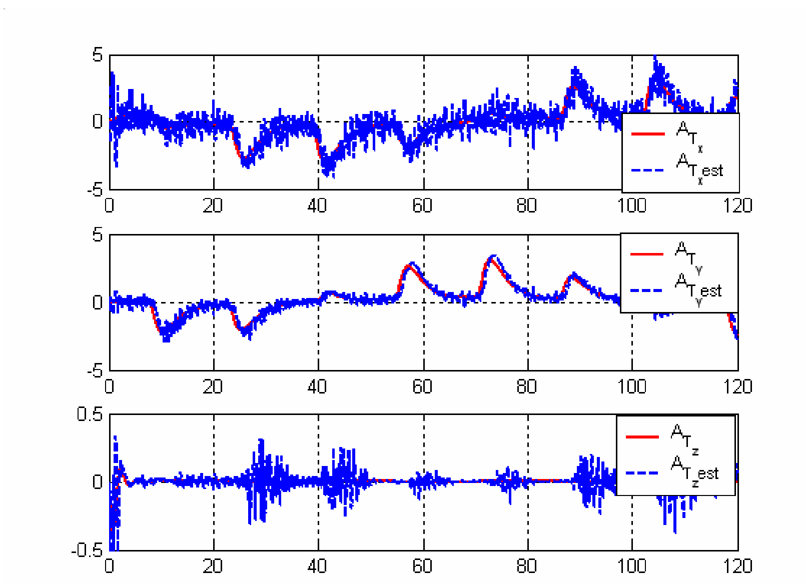

Figure 16. Target Acceleration Estimation, Circular Trajectory Maneuver, Adaptive Estimator formulated in this paper

V. Conclusion

We present an approach for augmenting a linear, time-varying Kalman filter with a neural network for the adaptive state estimation of SISO systems with linear process models in the presence of unknown but bounded system inputs. The approach combines two different error signals in the same adaptive law for the purpose of improving the adaptation performance. This is a composite adaptation approach to adaptive state estimation. The approach is applied to a target-tracking problem and simulation results clearly illustrate the benefits of incorporating an additional error signal in the adaptive law. The estimation of the target acceleration is reasonably very accurate and consistent for various target maneuvers.

Future research will include extending the approach developed in this paper to the adaptive state estimation of MIMO systems and systems with nonlinear process and measurement models. Secondly, we will study the issue of using the state estimates for the purpose of control. This is a much more challenging problem since we now cannot assume a priori that the outputs and inputs to the system are bounded and the adaptive estimation and control problems have to be treated in a unified manner. Finally, the adaptive estimation and control design will be integrated with image processing and evaluated in flight tests demonstrating vision-based formation flight between a maneuvering leader and follower aircraft.

Acknowledgments

This research has been sponsored under AFOSR contract F4960-01-1-0024 and under NRTC contract NCC 2-945. The authors also thank Konstantin Volyanskyy, Venkatesh Madyastha and Bong-Jun Yang for various technical interactions.

References

[1] Y. Bar-Shalom, X. R. Li, and T. Kirubarajan, *Estimation with Applications to Tracking and Navigation: Theory, Algorithms and Software,* Wiley-Interscience, New York, 2001.

[2] R.K Mehra, "On the Identification of Variances and Adaptive Kalman Filtering", *IEEE Transactions on Automatic Control,* AC-15, pp. 175-184, April 1970.

[3] A. Moghaddamjoo and R.L. Kirlin, "Robust Adaptive Kalman Filtering with Unknown Inputs", *IEEE Transactions on Acoustics, Speech and Signal Processing,* Vol. 37, No. 8, pp. 1166-1175, August 1989.

[4] M.E. Hough, "Improved Performance of Recursive Tracking Filters using Batch Initialization and Process Noise Adaptation", *AIAA Journal of Guidance, Control and Dynamics,* Vol. 22, No. 5, pp 675-681, 1999.

[5] R.A. Singer, "Estimating Optimal Tracking Filter Performance for Manned Maneuvering Targets", *IEEE Transactions on Aerospace and Electronic Systems,* AES-6, pp. 473-483, July 1970.

[6] Y. Bar-Shalom and K. Birmiwal, "Variable Dimension Filter for Maneuvering Target Tracking", *IEEE Transactions on Aerospace and Electronic Systems,* AES-18, pp. 621-629, 1982.

[7] H.A.P. Blom and Y. Bar-Shalom, "The Interacting Multiple-Model Algorithm for Systems with Markovian Switching Coefficients", *IEEE Transactions on Automatic Control,* AC-33, pp. 780-783, August 1988.

[8] J.A. Roecker and C.D. McGillem, "Target Tracking in Maneuver Centered Coordinates," *IEEE Transactions on Aerospace and Electronic Systems,* AES-25, pp. 836-843, November 1989.

[9] R.A. Best and J.P. Norton, "A New Model and Efficient Tracker for a Target with Curvilinear Motion," *IEEE Transactions on Aerospace and Electronic Systems,* AES-33, pp. 1030-1037, July 1997.

[10] M. Tahk and J.L. Speyer, "Target Tracking subject to Kinematic Constraints", *IEEE Transactions on Automatic Control,* AC-35, pp. 324-326, March 1990.

[11] X.R. Li and V.P. Jilkov, "Survey of Manuvering Target Tracking, Part I: Dynamic Models", *IEEE Transactions on Aerospace and Electronic Systems,* AES-39, pp. 1333 -1364, October 2003.

[12] Y.T. Chan, A.G.C. Hu and J.B. Plant, "A Kalman Filter based Tracking Scheme with Input Estimation", *IEEE Transactions on Aerospace and Electronic Systems,* AES-15, pp. 237-244, March 1979.

[13] P.L. Bogler, "Tracking a Maneuvering Target using Input Estimation", *IEEE Transactions on Aerospace and Electronic Systems,* AES-23, pp. 298-310, May 1987.

[14] H. Lee and M-J Tahk, "Generalized Input Estimation Technique for Tracking Maneuvering Targets", *IEEE Transactions on Aerospace and Electronic Systems,* AES-35, pp. 1388-1402, October 1999.

[15] K. Zhou, X. Wang, M. Tomizuka, W-B Zhang, and C-Y Chan, "A New Maneuvering Target Tracking Algorithm with Input Estimation", *American Control Conference,* pp. 166-171, May 2002.

[16] A.T. Alouani, P. Xia, T.R. Rice, and W.D. Blair, "Two-Stage Kalman Estimator for Tracking Maneuvering Targets", *IEEE International Conference on Systems, Man and Cybernetics,* pp. 761-766, October 1991.

[17] V.K. Madyastha and A.J. Calise, "An Adaptive Filtering Approach to Target Tracking", *American Control Conference,* pp. 1269-1274, June 2005.

[18] J-J E. Slotine and W. Li, *Applied Nonlinear Control*, Prentice Hall Inc., 1991.

[19] M.A. Duarte and K.S. Narendra, "Combined Direct and Indirect Approach to Adaptive Control", *IEEE Transactions on Automatic Control,* AC-34, pp. 1071-1075, October 1989.

[20] K. Volyanskyy, A.J. Calise and B-J Yang, "A Novel Q-Modification Term for Adaptive Control", accepted for publication in *American Control Conference,* 2006.

[21] H.K. Khalil, *Nonlinear Systems*, 2nd Edition, Prentice Hall Inc., 1996.

[22] E. Lavretsky, N. Hovakimyan and A.J. Calise, "Upper Bounds for Approximation of Continuous Time Dynamics using Delayed Outputs and Feedforward Neural Networks", *IEEE Transactions on Automatic Control,* AC-48, pp. 1606-1610, September 2003.

[23] R. G. Brown and P.Y.C. Hwang, *Introduction to Random Signals and Applied Kalman Filtering,* John Wiley and Sons Inc., 1992.

[24] K. Hornik, M. Stinchcombe and H. White, "Multi-Layer Feedforward Networks are Universal Approximators", *Neural Networks,* Vol. 2, pp. 359-366, 1989.

[25] K.S. Narendra and A.M. Annaswamy, "A New Adaptive Law for Robust Adaptation without Persistent Excitation", *IEEE Transactions on Automatic Control,* AC-32, pp. 134-145, 1987.

[26] R. Sattigeri, A. J. Calise, B.S. Kim, K. Volyanskyy and N. Kim, "6 DOF Nonlinear Simulation of Vision-based Formation Flight," *AIAA Guidance, Navigation, and Control Conference,* San Francisco, CA, August 2005.

[27] E. Johnson, A. Calise, R. Sattigeri, Y. Watanabe, and V. Madyastha, "Approaches to Vision-based Formation Control," *IEEE Conference on Decision and Control*, Vol. 2, pp 1643-1648, December 2004.
[28] V. Stepanyan and N. Hovakimyan, "Robust Adaptive Observer Design for Uncertain Systems with Bounded Disturbances," *IEEE Conference on Decision and Control*, pp 7750-7755, December 2005.